

The Application of Seismic Spectral Coherence to the Identification and Delineation of Stratigraphic Features in Niger Delta

Williams Ofuyah^{1*} Anthonia Asadu² Omafume Orji³ Stanley Eze⁴

1. Department of Earth Sciences, Federal University of Petroleum Resources, Effurun, Nigeria
2. Department of Earth Sciences, Federal University of Petroleum Resources, Effurun, Nigeria
3. Department of Petroleum Engineering and Geoscience, Petroleum Training Institute, Effurun, Nigeria
4. Department of Earth Sciences, Federal University of Petroleum Resources, Effurun, Nigeria

Abstract

Seismic spectral coherence images discontinuities by measuring lateral changes in the seismic response caused by variation in structure, stratigraphy, lithology, porosity and the presence of hydrocarbon, in terms of ratio of trace energies, in frequency domain. It operates on the seismic data itself. The aim of the study was to develop a robust technique for mapping subtle stratigraphic units. The methodology combined conventional coherence technique and non-conventional technique of the discrete Fourier transform. The geologic features were analyzed over a narrow time gate centered on the top of a thin sand interval. The response attribute maps, e.g. magnitude, phase, and frequency revealed hidden stratigraphic features.

Keywords: Discrete Fourier transform, Coherence, Semblance, Spectral decomposition

Introduction

The introduction of the 'coherence cube' by Bahorich and Farmer (1995) has resulted in the publication of new fault detection technologies describing the application of the technology using different algorithms with varying degrees of resolution capabilities. One of these papers by Marfurt et al (1998) on '3D seismic attributes using a semblance-based coherence algorithm received the award for the best paper in 1998, a testimony to the importance of this technology (Carter and Lines, 1999)

Seismic coherence images discontinuities by calculating localized seismic trace similarity (Peyton et al, 1998). It measures lateral changes in the seismic response caused by variation in structure, stratigraphy, lithology, porosity, and the presence of hydrocarbons (Marfurt et al 1998). Among the several advantages offered by seismic coherence are the ability to carefully analyze structural and stratigraphic features over an entire data volume including zones that are shallow, deep and adjacent to the primary zone of interest, identify and interpret subtle features that are not representable by picks on peaks, troughs, or zero-crossings, generate paleo-environmental maps of channels and fans corresponding to sequence versus reflector boundaries, etc (Marfurt et al 1998).

Spectral decomposition uses the discrete Fourier transform (DFT) to image thickness variability (Peyton et al, 1998). It provides a novel means of utilizing seismic data and DFT for imaging and mapping temporal bed thickness and geologic discontinuities over large 3D seismic surveys. By transforming the seismic data into the frequency domain via the DFT, amplitude spectra delineate temporal bed thickness variability, while the phase spectra indicate lateral geologic discontinuities. This technology has delineated stratigraphic settings like channel sands and structural settings involving complex fault systems in 3D seismic surveys (Partyka et al, 1999)

Seismic spectral coherence measures frequency response of computed amplitude-derived coherence data (time domain), as tuned by rock properties in the analysis window.

This paper presents the results of the application of coherence and spectral decomposition to the identification and delineation of stratigraphic features in the Niger delta. The aim was to delineate faults and subtle stratigraphic features and identify drilling prospects in the area of study which is known for its huge hydrocarbon potential.

Seismic coherence was computed from an extracted data volume integrating the zone of interest (sand interval) and along an arbitrary seismic line constructed to connect all six wells in the seismic survey. This was followed by the transformation of the results obtained in time into frequency using the DFT.

The main conclusion is that spectral decomposition of the conventionally computed coherence data enhances resolution capability, resulting in improved geologic maps. This has application in the localization of thin-bed reflections and definition of bed thickness variability within complex and rock strata including the detection of subtle discontinuities like facies change, channels, microfaults, reflection-free events within large 3D volume. The key inputs are the concepts and practices of seismic stratigraphy, principles of spectral decomposition, clear knowledge of signal analysis and thin-bed tuning phenomena and properly migrated seismic data.

Geologic Setting

The Niger delta is one of the most prolific oil producing areas in the world. It is located in southern Nigeria between latitudes 3°N and 6°N and longitudes $4^{\circ}30^{\prime}\text{E}$ and 9°E . The delta covers an area of about 105,000km². The Niger delta is a large arcuate delta of the destructive wave dominated type and is divided into the continental, transitional and marine environments. A sequence of under compacted marine shale (Akata formation, depth from 11121 ft) is overlain by paralic or sand/shale deposits (Agbada formation, depth from 7180-11121ft) is present throughout. Growth faults strongly influenced the sedimentation pattern and thickness distribution of sands and shales. The paralic interval is overlain by a varying thickness of continental sands (Benin formation, depth from 0-6000ft). Hydrocarbon is trapped in many different trap configurations. Oil and gas are trapped by roll-over anticlines and growth faults (Weber,1987). Merki(1972) noted that the age of the formations become progressively younger in a down-dip direction and ranges from Paleocene to Recent.

Seismic Data

The seismic data used in this study are digital and real. The recorded data sets (3D) were obtained by Chevron Corporation Nigeria. The field data comprises a base map , a suite of logs from six(6) wells, and four hundred (400) seismic lines and two hundred and twenty(220) crosslines . Some of the log types provided are Gamma-ray, self-potential, resistivity density, sonic, water saturation.

Seismic Coherence

Coherence is a measure of the similarity between waveforms or seismic traces. Coherence is defined as energy ratio which is normalized by total energy of the trace within the calculation window. For a large number of seismic traces, we could use the fact that when we stack several channels together, the resulting amplitude is generally large where the individual channels are similar (coherent) so that they stack in-phase and small where they are unlike (incoherent). The ratio of the energy of the stack compared to the sum of the energies of the individual components is a measure of the degree of coherence expressed as:

$$E_t = \frac{(\sum_i x_{ti})^2}{\sum_i (x_{ti}^2)} \quad (1)$$

where x_{ti} is the amplitude of the individual channel I at the time t, $\sum_i x_{ti}$ is the amplitude of the stack at time t and the square of this will be the energy. E_t is the ratio of the output energy to the sum of the energies of the input traces. (Telford et al,1985) The coherence algorithm attribute is designed to emphasize discontinuous events such as faults. Coherent event is expected to extend over a time interval with a high amplitude value on this attribute corresponding to discontinuities in the data, while a low amplitude value corresponds to continuous features.

Discrete Fourier Transform (DFT)

The Discrete Fourier Transform (DFT) is the digital equivalent of the continuous Fourier transform and is expressed as

$$f(w) = \sum_{t=-\infty}^{w-\infty} f(t) \exp(-iwt) \quad (2)$$

where, w is the Fourier dual of the variable 't'. If 't' signifies time, then 'w' is the angular frequency which is related to the linear (temporal frequency) 'f'. Also, F(w) comprises both real ($F_r(w)$) and imaginary $F_i(w)$ components. (Yilmaz, 2001).

Method

The main objective of our study was to develop a practical edge detection technique using coherence attribute for mapping subtle stratigraphy embedded in large 3D volume. This has the advantage of acting solely on the seismic data and is therefore devoid of horizon picker biases. The 2D data was extracted from the 3D volume along an arbitrary line created to tie the entire six wells in the survey.(i.e. for a thin sand/reservoir window with top: 2.752s, and base: 2.768s using Kingdom Suite software,. The extraction was done to enhance the hard data information and for detailed investigation of the inter-well regions to facilitate projection of result. In the spectral domain, DFT and fast Fourier transform (FFT) techniques were employed. Conventional Structural interpretation of 2D, and 3D data was also carried out with the Kingdom suite software, while the developed algorithm for coherence and its time-frequency transformation.(spectral decomposition) was achieved within Matlab software. Wells 01, 04 and 05 were adopted as representative wells for interpretation in view of their good data quality. Time slices (maps) of seismic amplitude at top and base of sand interval were computed. The stratigraphic features were analyzed over a narrow temporal window as defined by the maximum usable frequency (MUF) in the input seismic data. Coherence data (in terms of energy ratio of traces) was computed within a gate of $\pm 4\text{ms}$ centered on top of a conventionally interpreted sand interval in the seismic volume along

the arbitrary line. Gamma-ray amplitude map using three samples centered on top of sand in each well and across all six wells, following time-depth conversion, was also plotted. This was done to ensure adequate sampling rate of the insitu data to facilitate correlation. Finally, the horizon seismic amplitude slices (top and bottom), and corresponding GR amplitude and computed coherence data were transformed from time to frequency. The resulting response attribute maps (sand top) of amplitude; phase and frequency were plotted and compared with the original data in order to ascertain the resolving capacity of the coherence as an edge detection attribute and its maps in frequency domain. The GR map serves as reference map for sand and shale locations.

Discussion of Results

The results obtained are displayed as Figures 1 to 5. Figure 1 shows the arbitrary line after interpretation. Here, two major faults, F1, F2 are shown bounding the wells at the reservoir interval under analysis (2.752-2.768 seconds, arrowed). The well locations are indicated above the seismic section. In Figure 2, the zone of the arbitrary line is shown in relation to the seismic survey and the original Amplitude slice (Top of sand interval, 2.752 seconds). Figure 3 shows the amplitude and phase spectral plots by DFT at top of sand interval using different analysis window as follows: (a) GR plot, at 2.752s, using three samples per well centered at sand top were used for enhanced sampling,. Figure 3b is a display of the original amplitude plot at 2.752s while Figure 3c is the coherence plot (short window centered at 2.752s). The magnitude plot is symmetrical about the Nyquist frequency of 50Hz. The useful information in the signal is found in the range 0-50Hz. There is close resemblance of the edges at the 30 and 60Hz locations (i.e. F1, F2 on seismic section) in GR and coherence phase plots than on field data. The implication of this is that properly processed remotely sensed field data like seismic can approximate well or in-situ data.

The display in Figure 4, also at top of sand interval shows (a) Gamma-ray amplitude time map (b) Amplitude-Derived Coherence map. Note the enhanced image segmentation in the coherence (c) than in field amplitude (b). The shale lamination (light blue, high frequency) straddling the low frequency sand zone (green, yellow and orange are better delineated in (c) circled). The good well locations in the field data are the orange and brown segments (d), Detailed analysis indicate that wells 2,3 and 6 were sited on sand/shale interface. However the green location in (d) is a prospective zone by its low frequency anomaly..

Figure 5 is an integrated display of time and frequency attributes of GR, original seismic amplitude and coherence maps in the following order: (i) Gamma-ray amplitude time map and its corresponding frequency maps (b-e) and (ii) original amplitude map (a,f) and its corresponding coherence maps (g-j). Note the low GR amplitude and frequency values at the good well locations (green-orange). There is better edge definition at B (coherence) than at A (amplitude). The structural elements are more evident in the coherence maps than on the original amplitude data.

The coherence maps highlight the discontinuous events or edges such as faults. High amplitude values of coherence correspond to discontinuities in the data, while low amplitude values correspond to continuous features. Figure 5f is the amplitude (time) map and Figures 5g-j are the corresponding coherence time and frequency maps. Note that stratigraphic and structural elements like channel, faults were clearly unmasked in the discontinuity maps (e.g. Figure 5g) along the vertical axis of well 01 (circled). Coherence magnitude map (Figure 5h) highlights the main seismic features and represents the acoustic impedance contrast. It also reveals edges, changes in lithology, faults, and changes in deposition and sequence boundaries. The coherence phase (Figure 5i) indicates lateral continuity or sequence boundaries and also facilitates visualization of bedding discontinuities. The coherence frequency map (Figure 5j) shows correlation of the drilled zones with potential prospects (circled) by their low frequency anomaly. Higher frequencies indicate sharp discontinuities or thin shale. It also helps in identifying the edges of low impedance thin beds.

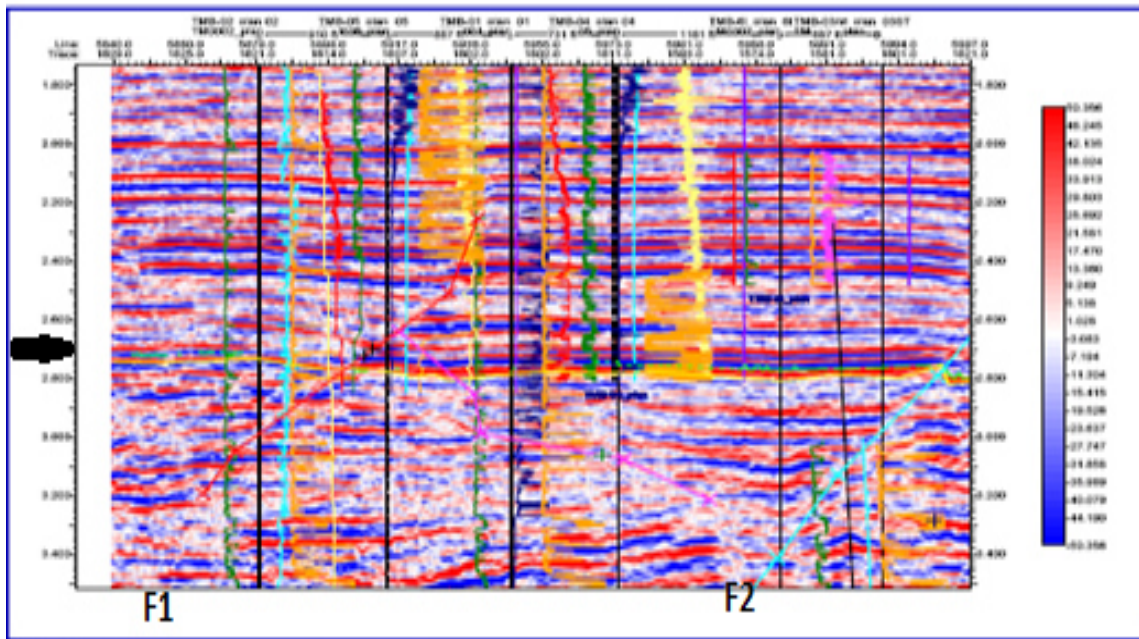


Figure 1 .Arbitrary line after interpretation: Two major faults, F1, F2 are shown bounding the wells at the reservoir interval under analysis (2.752-2.768 secs, arrowed).The well locations are indicated above the seismic section

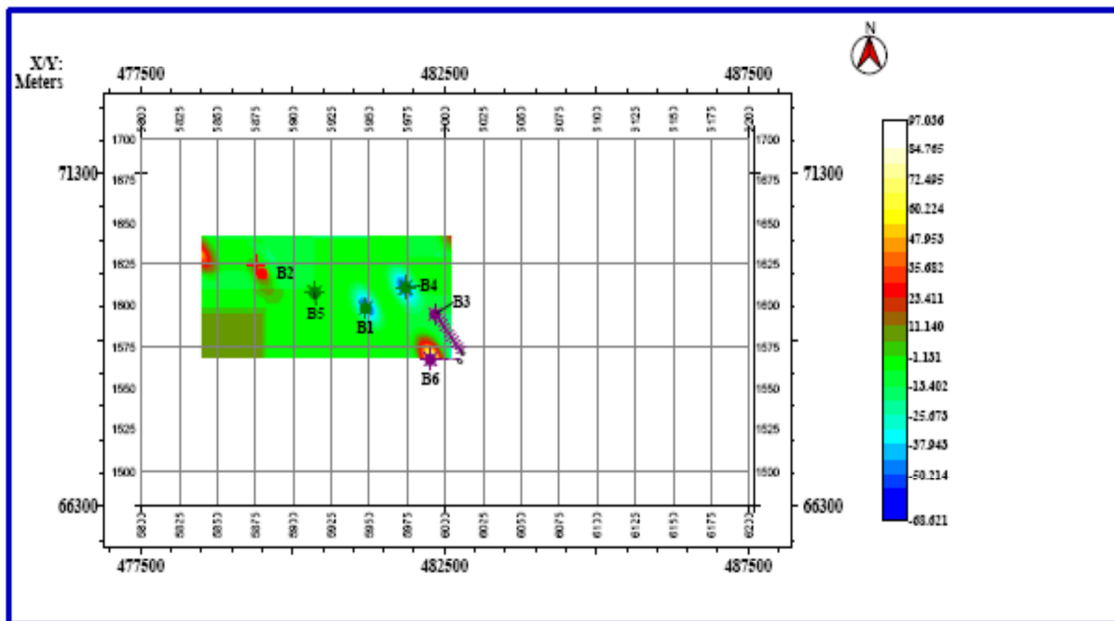
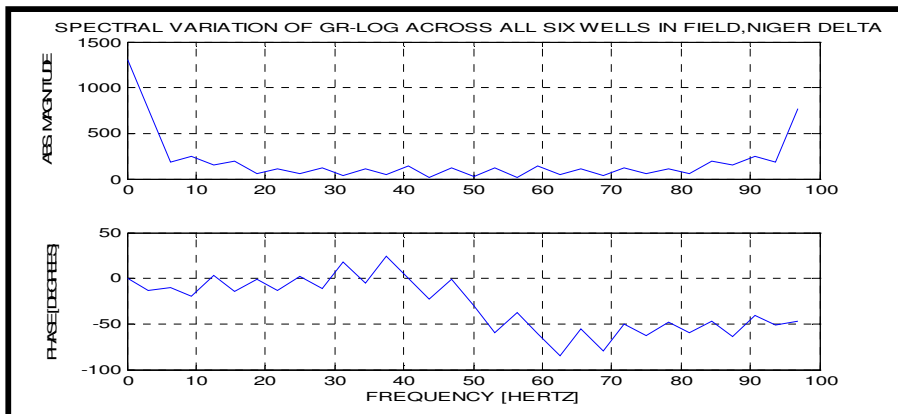
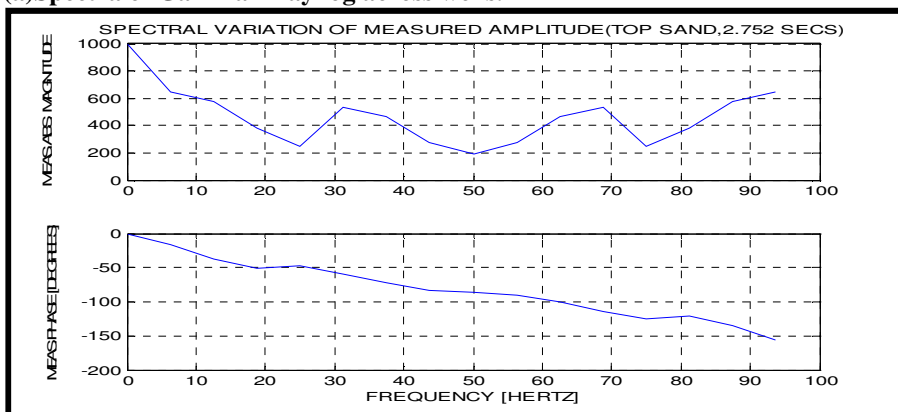


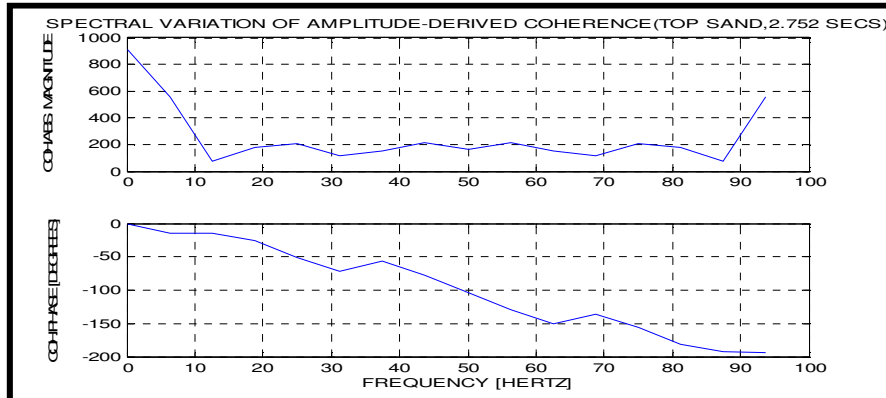
Figure 2: Zone of Arbitrary line in relation to the seismic survey and original amplitude map (Top of sand interval, 2.752 seconds).



(a) Spectra of Gamma –Ray log across wells.

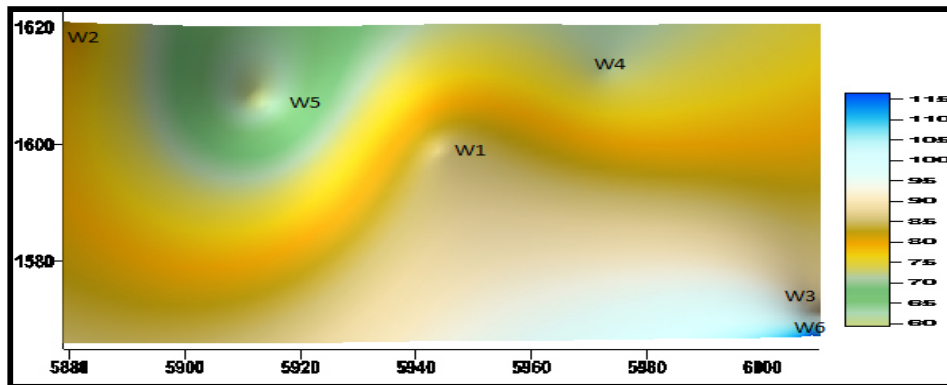


(b) Spectra of Measured Amplitude

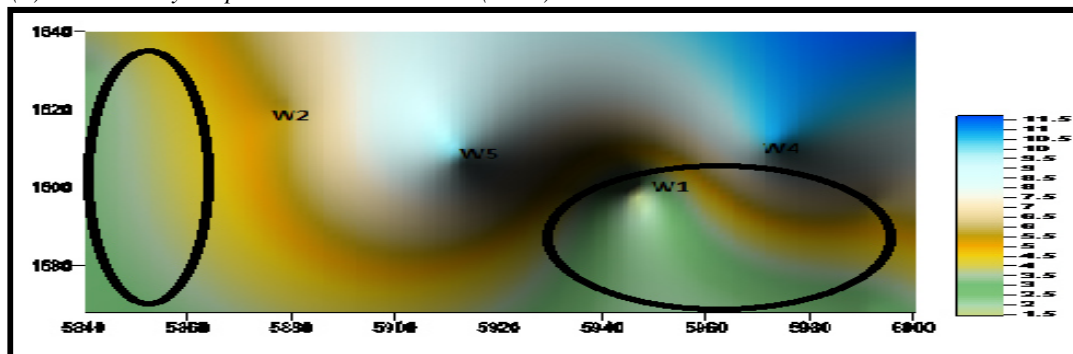


(c) Spectra of Amplitude-Derived Coherence.

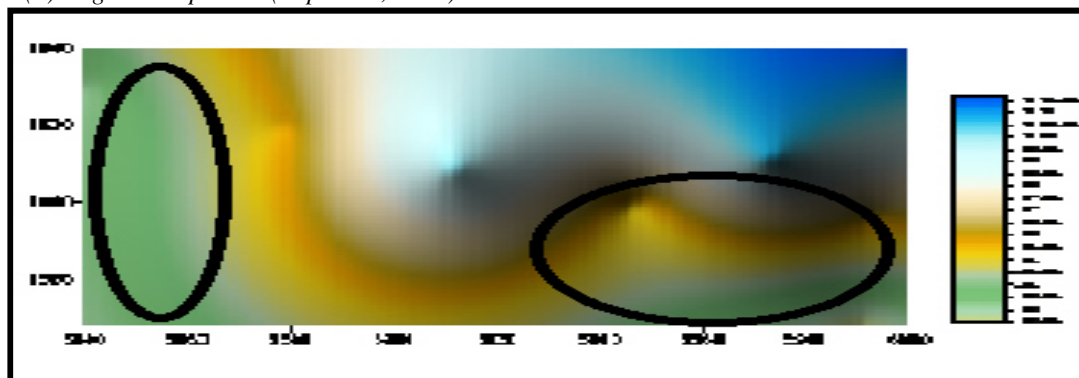
Figure 3: Amplitude and phase Spectral plots by DFT at top of sand interval (2.752seconds using same analysis window. (a)GR at 2.752s (three samples per well centered at sand top). (b) Original amplitude at 2.752s (c) coherence (short window centered at 2.752s). The magnitude plot is perfectly symmetrical about the Nyquist frequency of 50Hz..Compare the close resemblance of the edges at the 30Hz and 60Hz locations (i.e. F1, F2 on seismic section) in GR and coherence than in field data...



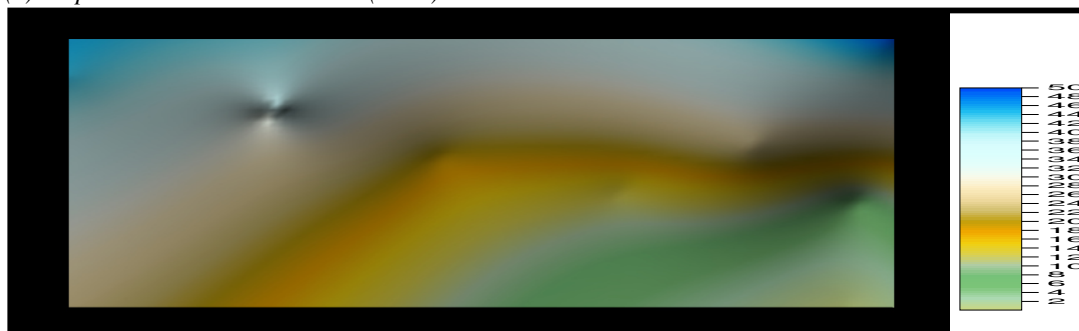
(a) Gamma-Ray Amplitude across six wells (Time)



(b) Original Amplitude (Top Sand, Time)



(c) Amplitude-derived Coherence (Time)



(d) Coherence Frequency

Figure 4: Top of sand (2.752 seconds): (a) Gamma-ray amplitude time map (b) Original amplitude map (c) Amplitude-Derived Coherence map (d) Coherence frequency. Note the enhanced image segmentation in the coherence than in field amplitude (b). The shale lination (light blue, high frequency) straddling the low frequency sand zone (green, yellow and orange) are better delineated in (c). The good well locations in the field data are the orange and brown zones (d). Wells 2,3 and 6 are on sand/shale interface. However the green location in (d) is a prospective zone (low frequency).

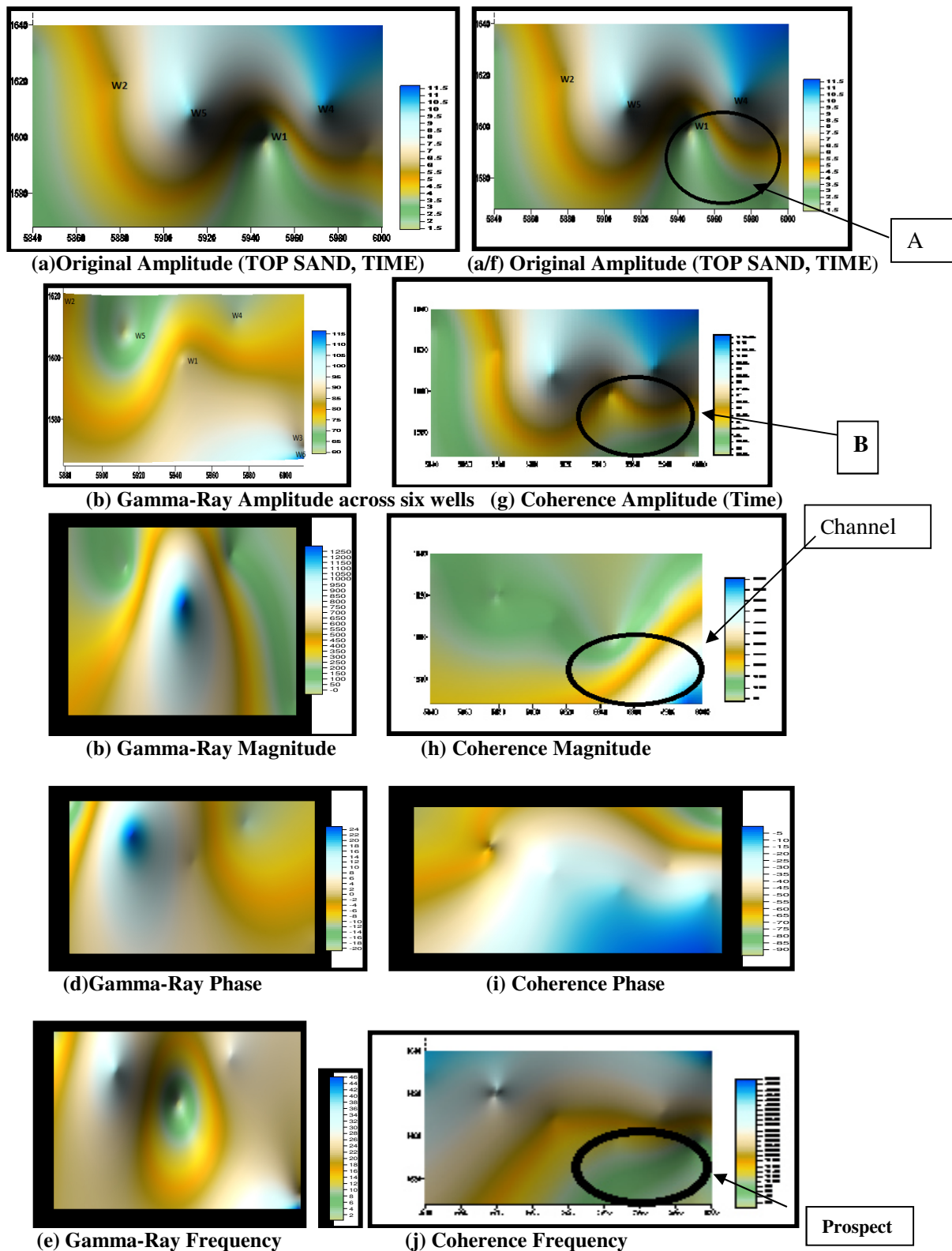


Figure 5: Top of sand (2.752 seconds): (i) Gamma-ray amplitude time map and its corresponding frequency maps (b-e) and (ii) Amplitude map(a,f) and its corresponding coherence maps (g-j). Note the low GR amplitude and frequency values at the good well locations (green-orange). There is better edge definition at B (coherence) than at A (amplitude). The stratigraphic and structural elements are more evident in the coherence maps than on the original amplitude data.

Conclusions

An investigation of the resolving capacity of the coherence attribute, computed in terms of energy ratio of traces has been undertaken. The analysis was initiated with field seismic amplitude data within a narrow window in time domain. The corresponding coherence attributes in frequency domain, using the discrete Fourier transform in the determination of lateral relations in our data were examined. The main objective of the study was to develop a robust technique for mapping subtle stratigraphic units which are usually masked after normal data interpretation using the edge detection technique of coherence which act on the seismic data itself and is devoid of horizon picker biases. The approach showed that computing a suite of coherence attributes in frequency domain rather than relying on traditional visualization of faults and channels from horizon picks, gives better results. The spectral coherency adopted gave improved geologic maps including information on potential prospective zones and paleo-environment corresponding to reflector boundary. The outputs of the algorithm revealed sub-seismic faults, discontinuities, channel, and amplitude/physical parameter transforms of the field. The reliability of the result is reinforced by its good correlation with Gamma-ray and other log data. This study has application in the localization of thin-bed reflections and the detection of subtle discontinuities like facies change, channels, microfaults, reflection-free events within dense 3D volume and complex rock strata. It is hoped that future work would adopt more sophisticated discontinuity attribute and compatible signal transform owing to the windowing limitations of the discrete Fourier transform.

Acknowledgements

We wish to thank Chevron Corporation, Nigeria for making the seismic and well data available for use. We are also indebted to Shell Nigeria for the use of the Kingdom Suite Software at its work station at Department of Geology, Obafemi Awolowo University (O.A.U.), Ile-Ife, Nigeria and to the Federal University of Petroleum Resources, Effurun, Nigeria for the use of her computing facilities.

References

- Bahorich, M.S., and Farmer, S.L. (1995): Seismic coherency for faults and stratigraphic features: The Leading Edge, pp 1053-1058
- Carter, N. and Lines, L.R. (1999): Fault imaging of Hibernia 3-D data using edge-detection and coherency measures, Crewes Research report, vol. 11
- Marfurt, K.J.; Sharp, J.A.; Scheet, R.M.; Ward, J.; Cain, C. and Harper, M.G. (1998): Suppression of the acquisition footprint for seismic attribute analysis, *Geophysics*, 68, pp 1024-1035
- Merki, P. J. (1972), Structural Geology of the Cenozoic Niger Delta. In: Dessauvage, T. F. J. and Whiteman, A. J. (eds), African Geology, University of Ibadan Press, Nigeria. pp. 635-646.
- Partyka, G.A., Gridley, J.M. and Lopez, J. (1999). Interpretational Applications of Spectral Decomposition in Reservoir Characterization. *The Leading Edge*, 18(3): 353-360.
- Taner, M.T., Koehler and Sheriff, R.E. (1979). Complex Trace Analysis, *Geophysics*, (44): 1041 – 1063. Revisited, 64th Annual International Meeting, SEG, Expanded Abstracts, 1104–1106.
- Telford, W.M.; Geldart, L.P.; Sheriff, R.E. and KEYS, D.A. (1985): *Applied Geophysics*, Cambridge University press, pp 393-396.
- Peyton, L., Bottjer, R. and Partyka, G., 1998, *Interpretation of incised valleys using new 3-D seismic techniques: A case history using spectral decomposition and coherency*. *The leading Edge*, 17, 1294-1298.
- Weber, K.J. (1987). *Hydrocarbon Distribution Patterns in Nigerian Growth Fault Structures Controlled by Structural Style and Stratigraphy*, *Journal of Petroleum science and Engineering*, 1: 91-104.
- Yilmaz O. (2001): *Seismic data analysis: processing, inversion, and interpretation of seismic data*: Society of Exploration Geophysicists, 2027 p.

List of Figures

Figure 1: Arbitrary line after interpretation: Two major faults, F1, F2 are shown bounding the wells at the reservoir interval under analysis (2.752-2.768 secs, arrowed). The well locations are indicated above the seismic section

Figure 2: Zone of Arbitrary line in relation to the seismic survey and original Amplitude map at top of sand interval, 2.752 secs).

Figure 3 : Amplitude and phase Spectral plots by DFT at top of sand interval (2.752 seconds) using different analysis window. (a) GR at 2.752s (three samples per well centered at sand top). (b) Original amplitude at 2.752s (c) coherence (short window centered at 2.752s). The magnitude plot is perfectly symmetrical about the Nyquist frequency of 50Hz..

Figure 4: Top of sand (2.752 seconds): (a) Gamma-ray amplitude time map (b) Original amplitude map (c) Amplitude-Derived Coherence map (d) Coherence frequency.

Figure 5: Top of sand (2.752 seconds): (i) Gamma-ray amplitude time map and its corresponding frequency maps (b-e) and (ii) Amplitude map (a,f) and its corresponding coherence maps (g-j).

The IISTE is a pioneer in the Open-Access hosting service and academic event management. The aim of the firm is Accelerating Global Knowledge Sharing.

More information about the firm can be found on the homepage:

<http://www.iiste.org>

CALL FOR JOURNAL PAPERS

There are more than 30 peer-reviewed academic journals hosted under the hosting platform.

Prospective authors of journals can find the submission instruction on the following page: <http://www.iiste.org/journals/> All the journals articles are available online to the readers all over the world without financial, legal, or technical barriers other than those inseparable from gaining access to the internet itself. Paper version of the journals is also available upon request of readers and authors.

MORE RESOURCES

Book publication information: <http://www.iiste.org/book/>

Academic conference: <http://www.iiste.org/conference/upcoming-conferences-call-for-paper/>

IISTE Knowledge Sharing Partners

EBSCO, Index Copernicus, Ulrich's Periodicals Directory, JournalTOCS, PKP Open Archives Harvester, Bielefeld Academic Search Engine, Elektronische Zeitschriftenbibliothek EZB, Open J-Gate, OCLC WorldCat, Universe Digital Library, NewJour, Google Scholar

